Effect of Nonsolvent on Morphologies of Polyamide 6 Electrospun Fibers

Wei Wei,[1] Jen-Taut Yeh,[2,3,4] Peng Li,[2] Min-Rui Li,[1] Wei Li,[5] Xin-Ling Wang[1]

[1]*Department of Polymer Science and Engineering, Shanghai Jiao Tong University, Shanghai 200240, China*
[2]*Department and Graduate School of Polymer Engineering, National Taiwan University of Science and Technology, Taipei, Taiwan*
[3]*Faculty of Material Science and Engineering, Hubei University, Wuhan, China*
[4]*Department of Textile and Material Engineering, Wuhan Textile University, Wuhan, China*
[5]*Instrumental analysis center of Shanghai Jiao Tong University, Shanghai 200240, China*

Received 15 February 2010; accepted 26 April 2010
DOI 10.1002/app.32704
Published online 1 July 2010 in Wiley InterScience (www.interscience.wiley.com).

ABSTRACT: The effect of nonsolvent on morphologies of electrospun polyamide 6 (PA6) fibers was reported in this study. An investigation of electrospinning PA6 / formic acid (FA) / dichloromethane (DCM) solutions was conducted, wherein FA was used as solvent and DCM was used as nonsolvent for PA6. It is interesting to note that PA6 pellets could dissolve in FA/DCM mixtures with various volume ratios faster than in pure FA. Moreover, the addition of DCM to PA6/FA solution modified the solution properties, that is, conductivity, surface tension, and viscosity. It is found that at any fixed PA6 concentration, the conductivity values and surface tensions values of PA6/FA/DCM solution reduce significantly, whereas the viscosity values of PA6/FA/DCM solution increase significantly, as the volume fraction of DCM in FA/DCM increase. The influences of mixed solvents component on morphological appearance and sizes of the resulting PA6 electrospun fibers were also investigated. © 2010 Wiley Periodicals, Inc. J Appl Polym Sci 118: 3005–3012, 2010

Key words: electrospinning; polyamide 6; nanofiber; formic acid; dichloromethane

INTRODUCTION

Electrospinning is an unconventional fiber spinning technology, which may produce nanofibers with diameters ranging from several microns to less than 10 nm. In electrospinning process, polymer nanofibers are continuously stretched from an electrostatically driven jet of polymer solution or polymer melt by the electrostatic repulsions. The nanofibers with small diameters and high-surface area show promise for the applications such as filtration,[1–3] drug delivery,[4] and tissue scaffolds.[5–8]

In view of the novel properties and functionalities of electrospun fibers, some investigations in preparing the nanofibers by electrospinning have drawn much attention for years.[9–25] It was found that the process parameters played important roles in determining morphology and sizes of the electrospun fibers obtained. These parameters include, (a) intrinsic properties of polymer solution such as concentration, conductivity, surface tension, polymer molecular weight, and solution temperature, (b) variety of solution system including the addition of other polymer and/or solvent, and (c) operational conditions such as applied electric field strength, fluid flow rate, nozzle diameter, spinneret-collector distance, and motion of the collector. With the control of these parameters, some nanofibers with interesting structures could be observed, such as beaded, porous and flat ribbon fibers.

Polyamide 6 (PA6) is one of the most important synthetic fiber-forming polymers. PA6 fibers with excellent toughness, wear, and thermal stability are widely used as wearing apparel, brush bristles, and carpet, which have been produced by conventional spinning techniques such as melt, wet, and dry spinning. However, fiber diameters produced by these spinning techniques are in the micron range about 10 to 500 μm. In view of the varying functional properties of nanofibers, investigations on producing submicron PA6 fibers have attracted some attentions by electrospinning. It was suggested that, the solution properties have a more dominant effect on the morphology and sizes of the electrospun fibers obtained.[9–18] Furthermore, solvent is one of the main contributors to polymer solution properties in addition to the contributor of intrinsic properties of polymer. It is worth noting that owing to presence of abundant hydrogen bondings among adjacent PA6 chains in both crystalline and amorphous regions,[19] formic acid (FA) is used mostly to dissolve PA6 in

Correspondence to: X.-L. Wang (xlwang@sjtu.edu.cn).

investigations.[9–13] Recently, the effects of solvent system on the electrospinning PA6 solutions and the morphological appearances of the resulting PA6 fibers were investigated by some authors.[9–14] Supaphol et al.[12] focused on three solvents (FA, *m*-cresol, and sulfuric acid) and the mixed solvent systems of binary blends of FA with another solvent (*m*-cresol, sulfuric acid, acetic acid, and ethanol). Among the investigated PA6 solutions in FA, *m*-cresol and sulfuric acid, only the PA6 solutions in FA produced smooth fibers. For the mix solvent systems investigated, all of the PA6 solutions in mixed solvents were spinnable and the average diameters of electrospun fibers were dependent on the properties of the PA6 solutions.

However, as far as we know, the effects of nonsolvent on the properties of PA6 solutions and the morphological appearance of the resulting fibers were ignored in most investigations. In 2007, Gogotsi and coworkers[14] reported a mix solvent of FA and dichloromethane (DCM) as a new solvent for dissolving PA 11 and PA 12 resins, which are the most difficult polyamides to dissolve in FA because of their long hydrocarbon chains. PA11 and PA12 can dissolve in a mixture of FA and DCM easily and can be electrospun to form nanofibers and nanoribbons. In contrast to Gogotsi's research, the effect of DCM as a nonsolvent for PA6 on electrospinning PA6/FA/DCM solution attracted our attentions, wherein FA was used as solvent and DCM was used as nonsolvent for PA6. It is expected that introducing of nonsolvent to solvent as a mix solvent should produce more interesting morphologies of electrospun fibers, as the varying component between nonsolvent and solvent. The influences of the mixed solvents component of DCM and FA on morphology and sizes of the electrospun PA6 fibers were investigated in this study. Furthermore, investigations including conductivity, surface tension, and viscosity experiments were performed accounting for the interesting morphology properties found for the PA6 nanofiber specimens.

EXPERIMENTAL

Preparation and characterization of PA6 solutions

PA6 used in this study was obtained from Formosa Chemicals Corporation (Taipei, Taiwan), wherein PA6 is nylon 6 with a trade name of Sunylon 6N. To prepare the electrospinning solutions, the PA6 pellets (1.14 g cm^{-3}) were dissolved in FA (88%, 1.23 g cm^{-3}) at room temperature with continuous stirring until transparent and homogeneous solutions were obtained. The effect of the solvent system on the obtained fibers was studied by using a mixture of FA and DCM (99.7%, 1.33 g cm^{-3}), in various volume ratios to prepare PA6 solutions. The boiling points of FA and DCM are 100.7°C and 39.7°C, respectively.

The conductivity, surface tension, and viscosity of the PA6 solutions were measured using a viscometer (NXS-11A, Chengdu Instrument Corp., Chengdu, China), conductivity meter (DDS-11D, Shanghai Precision & Scientific Instrument Corp., Shanghai, China), and a tensiometer (Krüss K12, Krüss instrument Corp. German) at room temperature (ca. 25°C) before electrospinning.

Dynamic light scattering

The chain dimensions of polymer chain coil in PA6 solutions were measured at 25°C using a dynamic light scattering (DLS) (Zetasizer Nano S, Malvern Instruments, Ltd., Worchestershire, U.K.), which equipped with a 4.0 mW He-Ne laser source operating at λ= 633 nm. The measurement range of this DLS apparatus is from 0.6 to 6000 nm. All samples were measured at a scattering angle of 173°.

Electrospinning

For electrospinning nanofibers, a voltage of 20 kV was applied to draw the nanofibers from the prepared solutions, by a high-voltage power supply. The desired PA6 solution was placed in a 6 mL syringe with a stainless steel needle (gauge number 22). A syringe pump was utilized to supply a constant droplet of solution at the tip of the needle. The flow rates were at 0.2 mL h^{-1} controlled by the syringe pump during electrospinning. A rotating drum collector covered with an aluminum foil was placed 20 cm horizontally from the tip of the needle and the fiber collector. All fiber spinning was done under ambient conditions.

Characterization of PA6 electrospun fibers

The morphologies of PA6 electrospun fibers were observed using a field emission scanning electron microscope (FESEM) (Siron200 200F, FEI, USA) at an accelerating voltage of 5KV. To provide electrical conductivity, each specimen was gold-coated using a JEOL E-1045 sputtering device before being observed under the SEM. The diameters of the nanofibers were determined from the FESEM image using the ImageJ software, and Origin 7.0 (OriginLab Corporation, Northampton, MA) was used for statistical data treatment.

RESULTS AND DISCUSSION

Solubility behavior of PA6 in FA and FA/DCM

The solubility of polymer in solvent can be predicted by means of solubility parameter (δ). For δ_m of

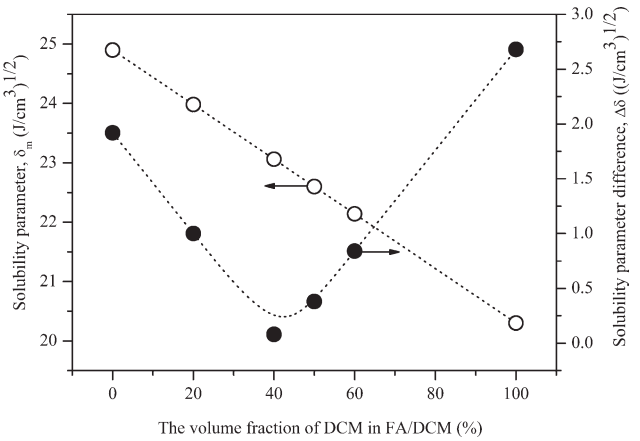

Figure 1 The δm values (○) and Δδ values (●) with varying the volume fraction of DCM in FA/DCM.

mixture, it is possible to express each of the solubility parameter components as: $\delta_m = \varphi_1\delta_1 + \varphi_2\delta_2$, wherein δ_m is the solubility parameter of mixture; φ_1 and φ_2 are the volume fractions of the components; δ_1 and δ_2 are the solubility parameters of the components. The calculated δ_m values of FA/DCM mixture at varying volume ratios according to above equation, and calculated Δδ (solubility parameter difference between PA6 and solvent) values at varying volume fractions of DCM in FA/DCM are shown in Figure 1. It is well-known that for PA6, FA with δ value of 24.9 is solvent, whereas DCM with δ value of 20.3 is nonsolvent. Noting that the δ_m values reduced from 23.98 to 22.14 as the volume fractions of DCM increased from 20 to 60%, which were all close to the δ value of PA6 (22.9). Moreover, all Δδ values were below 1.5 as the volume fractions of DCM ranged from 20–60% and the minimum Δδ value occurred as the volume fraction of DCM was 40%. These results indicate PA6 could dissolve in FA/DCM mixture.

Figure 2 exhibits the dissolution of PA6 pellets in FA, F80D20, F60D40, F50D50, and F40D60 observed after PA6 solution stirred at 250 r min^{-1} and 30°C for 0, 40, and 80 min, respectively. It is interesting to find that all PA6 solutions appeared transparent after stirried at 250 r min^{-1} and 30°C for 80 min and could be stable over time, indicating that PA6 pellets could dissolve completely in volume ratios ranging from 100/0 to 40/60 of FA/DCM. However, FA/DCM mixtures with various volume ratios lead to faster dissolution of PA6 pellets than pure FA. In addition, F60D40 shows the fast dissolution of PA6 pellets in these FA/DCM mixtures with various volume ratios [see Fig. 2 (40 min)]. The experimental observations are in good agreement with the results predicted by solubility parameter. However, these results are slightly in disagreement with Gogotsi's and cowrkers article,[14] wherein he reported pure FA to 60/40 (FA/DCM) volume ratio mixtures led to rapid dissolution of the PA6 pellets while higher ratios (including 50/50) did not dissolve the PA6 pellets. It is not clear what accounts for these interesting disagreement in dissolution observed from PA6 dissolving in FA/DCM. Interestingly, it is further to observe that PA6 solutions exhibit from homogenous to inhomogeneous as the volume ratios of FA and DCM vary from 60/40 [see Fig. 3(a)] to 50/50. As the volume ratio of FA and DCM varying to 40/60, liquid-liquid demixing appears in PA6/ F40D60 solution stable to long time [see Fig. 3(b)]. Presumably, as the volume ratio of FA and DCM is equal to and more than 50/50, the solubility of DCM in FA decreases and excess DCM deposits in the bottom of the vial owing to its higher density. Therefore, 40% DCM in

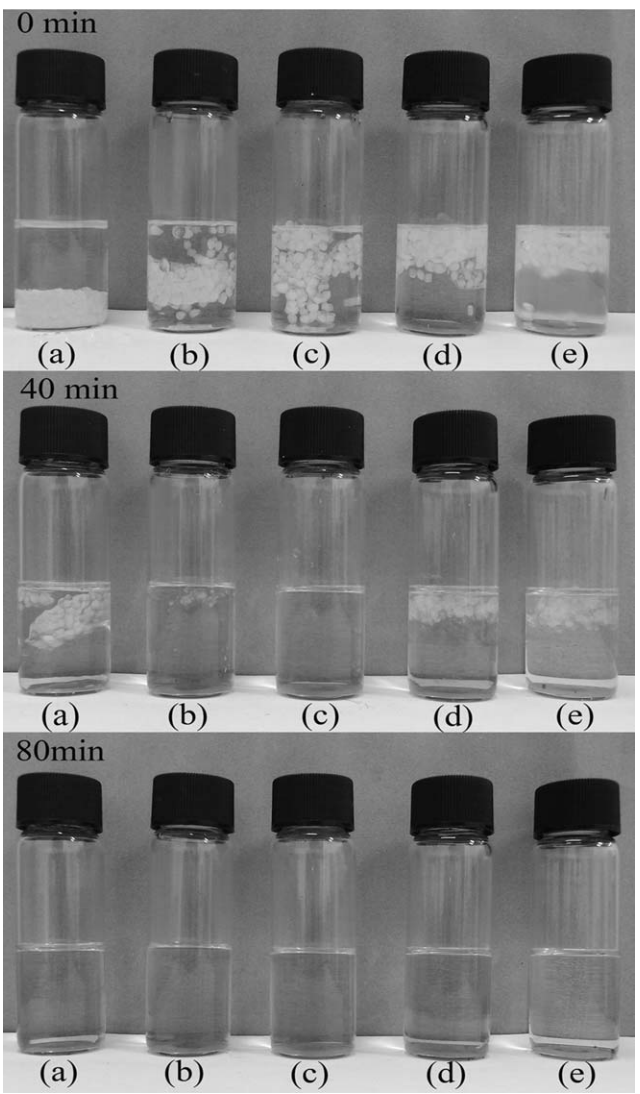

Figure 2 Photographs of PA6 solutions of PA6 pellets (2 g) dissolved in solvents (10 mL) of (a) FA, (b) F80D20, (c) F60D40, (d) F50D50, and (e) F40D60 obtained after PA6 solutions stirred at 250 r min^{-1} and 30°C for 0, 40, and 80 min, respectively.

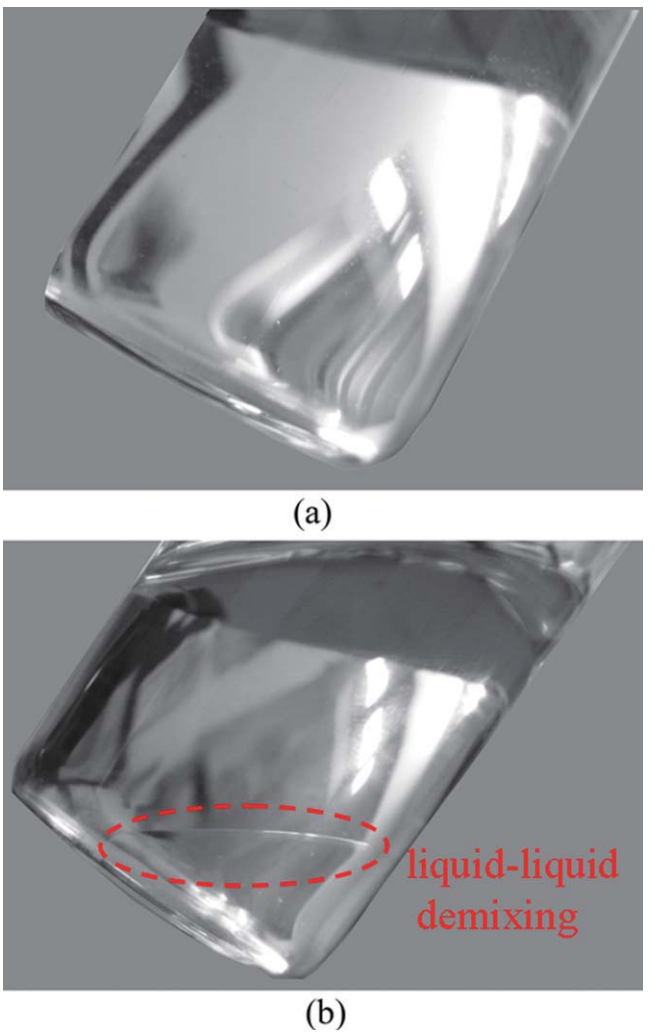

Figure 3 Photographs of 20% w/v PA6 solution in mixed solvents of (a) F60D40 and (b) F40D60. [Color figure can be viewed in the online issue, which is available at www.interscience.wiley.com.]

FA/DCM as the maximum volume fraction is adopted in the following experiments.

The chain dimensions of polymer chain coil in PA6 solutions were measured by DLS. Generally, dilute polymer solutions are measured in DLS measurement. When concentration is increased, there occurs destructive interference between the waves scattered from the different solute particles in concentrated solution. Therefore, 8 % w/v PA6/FA and PA6/$F_{60}D_{40}$ solution specimens were measured in this study. As shown in Figure 4, the average diameter of PA6 coil in PA6/FA solution is about 1.85 nm, whereas that in PA6/$F_{60}D_{40}$ solution reduces to 1.72 nm. It is generally recognized that the interactions of molecular chains present repulsion and the polymer chain coils are slack in solvent, whereas the gravitations of molecular chains increase and the polymer chain coils shrink after adding nonsolvent to solvent. On the basis of these premises, it is reasonable to believe that the average diameter of PA6 chain coils in PA6/FA solution is higher than that in PA6/$F_{60}D_{40}$ solution.

Properties of the PA6 solutions

In electrospinning a polymer solution, various solution properties (viscosity, conductivity, and surface tension, etc.) play an important role in the morphology of the obtained electrospun fibers. The viscosity, surface tension and conductivity values for PA6/FA, PA6/$F_{80}D_{20}$, and PA6/$F_{60}D_{40}$ solutions at various PA6 concentrations are summarized in Figures 5 to 7. As shown in Figure 5, the viscosity values of PA6/FA, PA6/$F_{80}D_{20}$, and PA6/$F_{60}D_{40}$ solutions increase tremendously with the increasing PA6 concentrations, respectively. In fact, as PA6 concentrations increase from 8 to 40 % w/v, the viscosity values of PA6/FA solutions were found to increase from 62.4 to 13,601 cp, whereas the viscosity values of PA6/$F_{80}D_{20}$ and PA6/$F_{60}D_{40}$ solutions were found to increase from 69.5 to 13,885 cp and from 101.44 to 14,032 cp, respectively. These results obtained can be explained that the tremendous increase of the solution viscosity may be attributed to the increased number of molecular chain entanglements with the increasing PA6 concentrations, and then demonstrate an increase in the viscoelastic force of polymer solution. It is interesting to note that at any fixed PA6 concentration, the viscosity values of PA6/FA, PA6/$F_{80}D_{20}$, and PA6/$F_{60}D_{40}$ exhibit increase consistently with the increasing volume fractions of DCM in FA/DCM. For instance, the viscosity values for PA6/FA/DCM solutions at the PA6 concentration of 25% w/v increase from

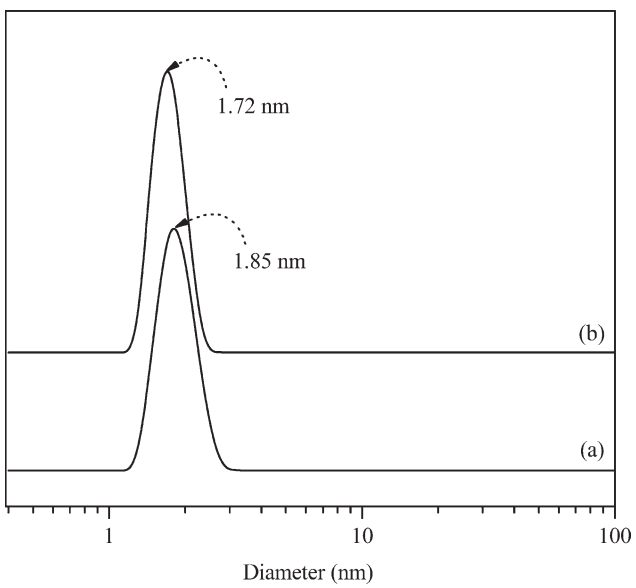

Figure 4 A typical DLS plot of 8% w/v (a) PA6/FA and (b) PA6/F60D40 solution specimens determined at 25°C.

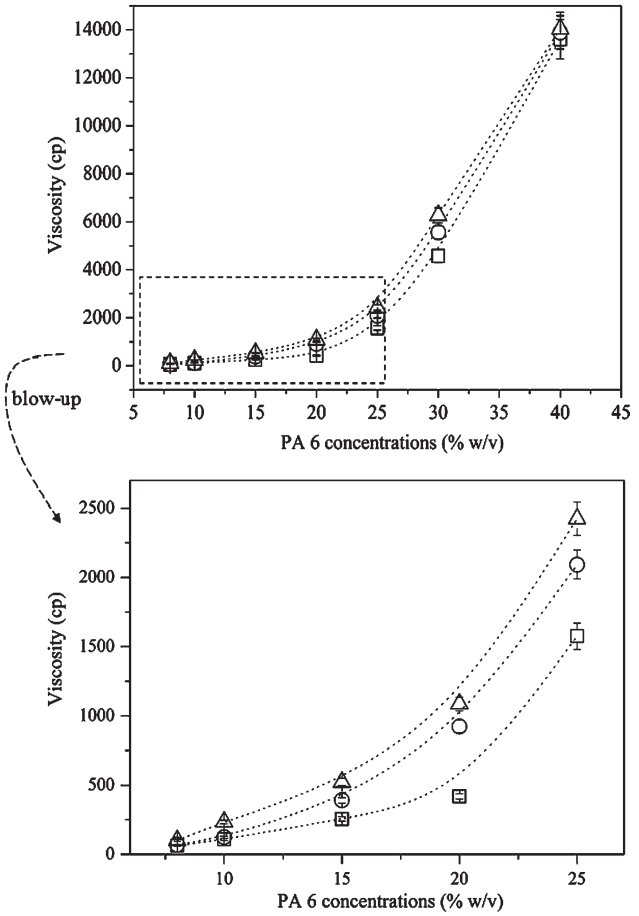

Figure 5 The viscosity of PA6/FA (□), PA6/F80D20 (○), and PA6/F60D40 (△) solutions with varying PA6 concentrations.

1576.3 to 2091.9 and then to 2424.4 cp, as volume fractions of DCM in FA/DCM increase from 0 to 20 and 40%, respectively. As evidenced by the analysis of DLS, addition of DCM to PA6/FA solution produced the shrink of polymer chain coils, and hence,

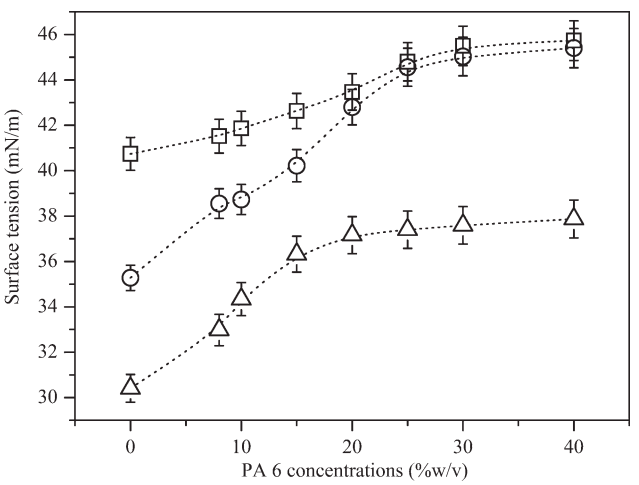

Figure 6 The surface tension of PA6/FA (□), PA6/F80D20 (○), and PA6/F60D40 (△) solutions with varying PA6 concentrations.

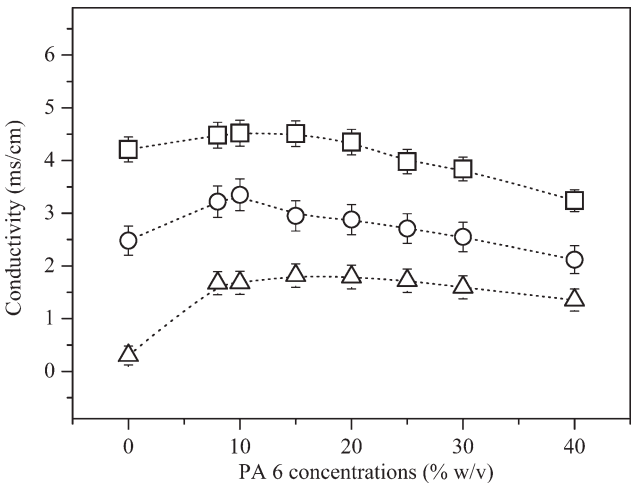

Figure 7 The conductivity of PA6/FA (□), PA6/F80D20 (○), and PA6/F60D40 (△) solutions with varying PA6 concentrations.

to results in more chain entanglements. As a consequence, at any fixed PA6 concentration, the viscosity values of PA6/FA/DCM present increase consistently with the increasing volume fractions of DCM in FA/DCM.

Figure 6 shows the surface tension values of PA6/FA, PA6/$F_{80}D_{20}$, and PA6/$F_{60}D_{40}$ solutions at various PA6 concentrations. It is found that the surface tension values of PA6/FA, PA6/$F_{80}D_{20}$, and PA6/$F_{60}D_{40}$ solutions increase gradually with increasing PA6 concentrations ranging from 0 to 40% w/v, respectively. As shown in Figure 7, as the PA6 concentrations increase from 0 to 40 % w/v, the surface tension values for PA6/FA solutions increase from 40.7 to 45.7 mN m^{-1}, whereas the surface tension values of PA6/$F_{80}D_{20}$ and PA6/$F_{60}D_{40}$ solutions increase from 35.2 to 45.4 mN m^{-1} and from 30.4 to 37.9 mN m^{-1}, respectively. However, it is worth noting that at any fixed concentration, the surface tension values of PA6 solutions reduce as the volume fractions of DCM in FA/DCM increase. Apparently, the surface tension values for PA6/FA/DCM solutions at the concentration of 30% w/v reduce from 45.5 to 45 and then to 37.5 mN m^{-1}, as volume fraction of DCM in FA/DCM increase from 0 to 20 and 40%, respectively. One possible account is that the increasing entanglements between macromolecular chains of PA6 in solutions can cause the increase in surface tensions, as PA6 concentrations increase. Moreover, the addition of DCM with low surface tensions has a significant effect on reducing the surface tensions of FA/DCM mixtures. Obviously, the values for FA/DCM decrease significantly from 40.7 to 35.2 and then to 30.4 mN m^{-1}, as the volume fractions of DCM in FA/DCM increase from 0 to 20 and 40% (see Fig. 6).

The conductivity values of PA6/FA solutions were found to increase initially with increasing PA6 concentrations, and then approach a maximum

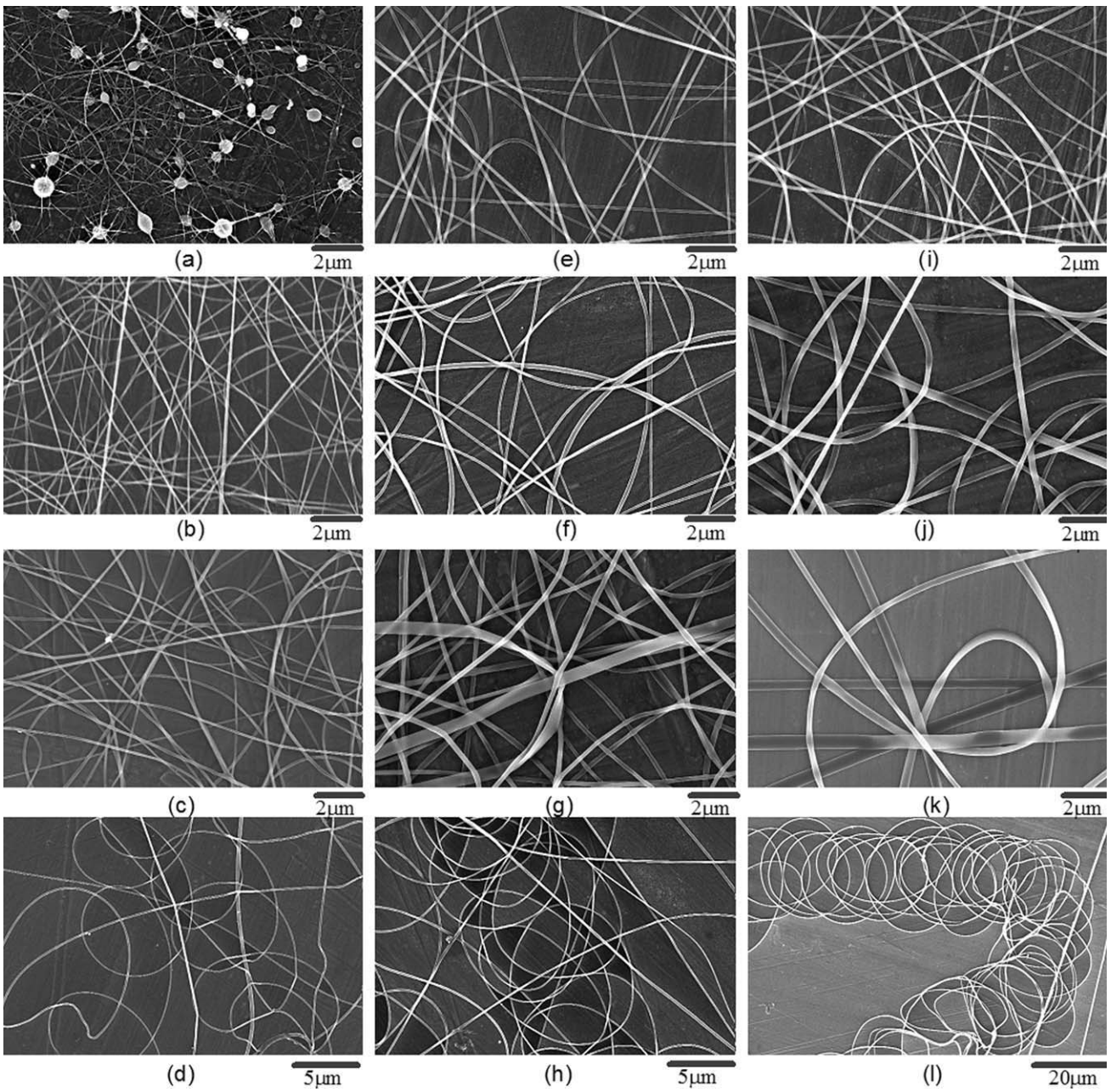

Figure 8 SEM images of electrospun (a) 10% w/v PA6/FA, (b) 15% w/v PA6/FA, (c) 25% w/v PA6/FA, (d) 30% w/v PA6/FA, (e) 10% w/v PA6/F80D20, (f) 15% w/v PA6/F80D20, (g) 25% w/v PA6/F80D20, (h) 30% w/v PA6/F80D20, (i) 10% w/v PA6/F60D40, (j) 15% w/v PA6/F60D40, (k) 25% w/v PA6/F60D40, and (i) 30% w/v PA6/F60D40 fiber specimens.

value, as the PA6 concentrations are close to the 10% w/v optimum value (see Fig. 7). At the PA6 concentrations higher than 10% w/v, the conductivity values reduce reversely with the further increase in PA6 concentrations. In fact, the conductivity values for PA6/FA solutions increase from 4.2 to 4.5 and then to 3.2 ms cm^{-1}, as the PA6 concentrations increase from 0 to 10 and 40% w/v, respectively. Similarly, the conductivity values of $PA6/F_{80}D_{20}$ and $PA6/F_{60}D_{40}$ solutions are found to approach a maximum value (e.g. 3.3 and 1.7 ms cm^{-1}), as the PA6 concentrations are close to about 10 and/or 15% w/v optimum value, respectively. Moreover, at any fixed concentration, the conductivity values of PA6 solutions reduce as the volume fractions of DCM in FA/DCM increase. For instance, the conductivity values for PA6/FA /DCM solutions at the PA6 concentration of 10% w/v reduce from 4.5 to 3.3 and then to 1.7 ms cm^{-1}, as volume fractions of DCM in FA/DCM increase from 0 to 20 and 40%, respectively. As the PA6 concentrations are equal to or less than 10% w/v, free C=O functional groups of PA6 macromolecule chains dissolving completely in FA could presumably improve the transferability of moving ions in solution.

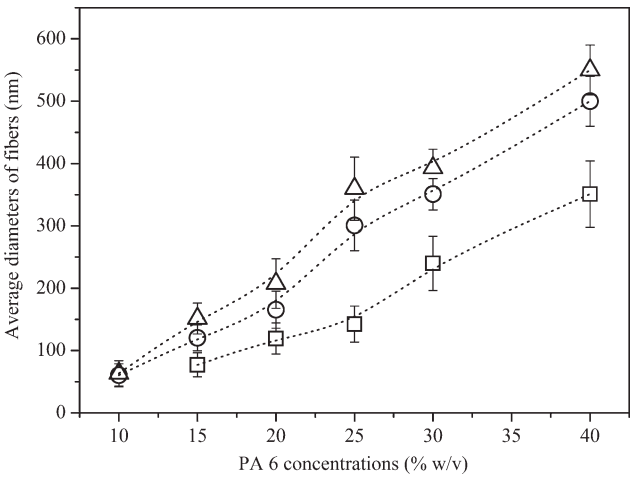

Figure 9 Average diameters of electrospun PA6/FA (□), PA6/F80D20 (○), and PA6/F60D40 (△) fibers with varying PA6 concentrations.

The numbers of chain entanglements are expected to increase as the viscosity increase. It is, therefore, reasonable to understand that as the PA6 concentrations increase, the significantly increased numbers of molecular chain entanglements may disturb the movement of ions in PA6 solutions and thus reduce the conductivity values of PA6 solutions. However, the amounts of moving ions in PA6/FA/DCM reduce significantly as the volume fractions of DCM with low conductivity increase. As a consequence, at any fixed concentration, the conductivity values of PA6/FA/DCM solution reduce significantly as the volume fractions of DCM in FA/DCM increase.

Morphologies of PA6 electrospun fibers

Typical SEM micrographs of nanofibers electrospun from PA6/FA, PA6/$F_{80}D_{20}$, and PA6/$F_{60}D_{40}$ solutions are shown in Figure 8. On electrospinning PA6/FA solutions, it was found that the spinnability would be poor and nanofibers with beads are formed at the concentrations lower than 10%w/v [see Fig. 8(a)]. At PA6 concentrations higher than 10% w/v, beads disappear and smooth fibers with cylindrical cross-section are obtained [see Fig. 8(b–d)]. However, a large number of fibers formed loops, as the PA6 concentrations increased to 30% w/v [see Fig. 8(h,i)], indicating the electrical bending instability. Apparently, the diameters of electrospun nanofibers increase as PA6 concentrations increase. As shown in Figure 9, the average diameters of electrospun nanofibers increase from 77 to 350 nm with the PA6 concentrations increasing from 15 to 40% w/v. Furthermore, the nonuniformity of electrospun nanofibers indicated by the error bars increases with the increasing PA6 concentrations. During electrospinning, three most important forces (i.e. viscoelastic force, Coulombic force, and surface tension) are responsible for the formation of electrospun fibers.[10,26] As evidenced by analysis of the properties of PA6 solutions in the previous section, the viscoelastic forces and surface tensions were found to increase with increasing PA6 concentrations, whereas the Coulombic force approached the maximum as PA6 concentration was about 10%. At the concentrations lower than 10% w/v (equivalent to a viscosity value of about 108 cp), the viscoelastic force which prevents the charged jet from stretching could be presumably smaller than the Coulombic force stretching the charged jet. Therefore, the charged jets were over stretched to break up into small droplets. Then surface tension in droplets created a pressure that forced them to form beads. The fibers with beads were obtained on the target collector or even dripping of polymer solution occurred during the electospinning. As the concentrations increase to 15% w/v (about 255 cp), the effects of surface tension and Coulombic force on the fluid jet reduce, whereas the viscoelastic forces increase. The viscoelastic forces prevented the charged jet breaking up into small droplets and smooth bead-free fibers were formed. As the concentrations are equal to and more than 30% w/v (about 4570 cp), the viscoelastic forces have the dominant influence on the formation of electrospun fibers. As a consequence, the average diameters and the nonuniformity of electrospun fiber specimens increase significantly with the increasing PA6 concentrations.

As shown in Figure 8(e–i), the influences of the mixed solvents component of DCM and FA on morphology of the obtained PA6 electrospun fibers were investigated by electrospinning PA6/$F_{80}D_{20}$ and PA6/$F_{60}D_{40}$ solutions. In contrast to fibers with beads electrospun from 10% w/v PA6/FA solution [see Fig. 8(a)], smooth nanofibers without beads were observed in electrospinning 10% w/v PA6/$F_{80}D_{20}$ and PA6/$F_{60}D_{40}$ solutions, respectively [see Fig. 8(e,i)], indicating that the rapid evaporation of FA/DCM benefited the formation of electrospun fiber on the streching of charged jet. As the PA6 concentrations were less than 25% w/v, a large proportion of electrospun fibers presented elliptical [see Fig. 8(f,j)]. Interestingly, flat ribbon-shaped electrospun fibers were produced as the PA6 concentration was close to 25% w/v [see Fig. 8(g,k)], whereas bending loops were formed instead of ribbon-like fibers, as the PA6 concentrations increased to 30% w/v [see Fig. 8(h,i)]. Moreover, the average diameters of fiber specimens electrospun from PA6/$F_{80}D_{20}$ solution increase from 60 to 500 nm with PA6 concentrations increasing from 10 to 40% w/v (see Fig. 9). Apparently, at any fixed PA6 concentrations, the average diameters of electrospun fibers were found to increase with the increasing volume fractions of DCM in FA/DCM, likely a result of the increased viscosity and the decreased conductivity values. The nonuniformity of electrospun nanofibers indicated by the error bars increases consistently with the increasing volume fractions of DCM in

FA/DCM at fixed PA6 concentrations. It is not clear what accounts for these interesting morphology properties observed for PA6/FA/DCM electrospun fiber specimens. However, it is generally recognized that these morphologies are most likely related to the formation of fiber skin-core structure. As mentioned above, the boiling point of FA (100.7°C) is much higher than that of DCM (39.7°C). Presumably, the skin and core layers of polymer fiber were almost formed together at low PA6 concetration (e.g. 10% w/v) with the rapid evaporation of FA/DCM. As the concentration increased from 10% w/v to 25% w/v, a thin polymer skin on the charged jet was formed first owing to the difference of solvent evaporation between the surface and core of the jet. Then, atmospheric pressure tended to shrink or collapse the tube formed by the skin as evaporation of solvent inside. However, as the concentrations increase, the charge density of charged jet decrease and the viscoelastic forces increase significantly. The electrospun fiber could not be stretched to form thin nanofiber by Coulombic force. Therefore, on the various complicate interactions the circular initially cross-section of electrospun fiber showed cylindrical to elliptical and then to flat as the solvent evaporated. Furthermore, as the concentrations increase to 30% w/v, the stiffness of the skin on the charged jet were formed first and prevented the tube to collapse, and hence, to result in the bending loops owing to the electrical bending instability.

CONCLUSIONS

In this study, the electrospinning of PA6 /solvent/ nonsolvents was reported, wherein FA was used as solvent and DCM was used as nonsolvent for PA6. On electrospinning the PA6/FA solutions, nanofibers with beads were formed at the concentration lower than 10% w/v, whereas smooth fibers without beads were obtained at the concentrations higher than 10% w/v. The average diameters of electrospun nanofibers increase from 77 to 350 nm with the PA6 concentrations increasing from 15 to 40% w/v. It is worth noting that as evidenced by the analysis of DLS, addition of DCM to PA6/FA solution produced the shrink of polymer chain coils. As a consequence, at any fixed PA6 concentration, the conductivity and surface tension values of PA6/FA/DCM solutions decreased and the viscosity values of PA6/FA/DCM solutions increased consistently with increasing volume fractions of DCM in FA/DCM, respectively. On electrospinning the PA6/$F_{80}D_{20}$ and PA6/$F_{60}D_{40}$ solutions, smooth nanofibers without beads were observed at the PA6 concentration of 10% w/v. As the PA6 concentrations were less than 25% w/v, a large proportion of electrospun fibers presented elliptical. It is interesting to note that the flat ribbon-shaped electrospun fibers were obtained as the concentration was 25% w/v, whereas ribbon-like fibers disappeared completely, as the concentrations increase to 30% w/v. The skin-core structure of fibers caused by the difference of solvent evaporation between the surface and core of the charged jet mainly contributed to the development in morphologies of fibers electrospun from PA6/$F_{80}D_{20}$ and PA6/$F_{60}D_{40}$ solutions. The average diameters of fiber specimens electrospun from PA6/$F_{80}D_{20}$ solution increase from 60 to 500 nm with PA6 concentrations increasing from 10 to 40% w/v. Furthermore, at any fixed PA6 concentrations, the average diameters of electrospun fibers were found to increase with the increasing volume fractions of DCM in FA/DCM, likely a result of the increased viscosity and the decreased conductivity values.

References

1. Gopal, R.; Kaur, S.; Ramakrishna, S. J Membr Sci 2006, 281, 581.
2. Barhate, R. S.; Ramakrishna, S. J Membr Sci 2007, 296, 1.
3. Heikkila, P.; Taipale, A.; Lehtimaki, M.; Harlin, A. Polym Eng Sci 2008, 48, 1168.
4. Kenawy, E. R.; Bowlin, G. L.; Mansfield, K. J Controlled Release 2002, 81, 57.
5. Ma, Z.; Kotaki, M.; Inai, R.; Ramakrishna, S. Tissue Eng 2005, 11, 101.
6. Barnes, C. P.; Sell, S. A.; Boland, E. D. Adv Drug Delivery Rev 2007, 59, 1413.
7. Liang, D.; Hsiao, B. S.; Chu, B. Adv Drug Delivery Rev 2007, 59, 1392.
8. Li, W. J.; Laurencin, C. T.; Caterson, E. J.; Tuan, R. S.; Ko, F. K. J Biomed Mater Res 2002, 60, 613.
9. Mit-Uppatham, C.; Nithitanakul, M.; Supaphol, P. Macromol Chem Phys 2004, 205, 2327.
10. Mit-Uppatham, C.; Nithitanakul, M.; Supaphol, P. Macromol Symp 2004, 216, 293.
11. Supaphol, P.; Mit-Uppatham, C.; Nithitanakul, M. J Polym Sci Part B: Polym Phys 2005, 43, 3699.
12. Supaphol, P.; Mit-Uppatham, C.; Nithitanakul, M. Macromol Mater Eng 2005, 290, 933.
13. Gupta, A.; Saquing, C. D.; Kotek, R. Macromolecules 2009, 42, 709.
14. Behler, K.; Havel, M.; Gogotsi', Y. Polymer 2007, 48, 6617.
15. Reneker, D. H.; Chun, I. Nanotechnology 1996, 7, 216.
16. Fong, H.; Chun, I.; Reneker, D. H. Polymer 1999, 40, 4585.
17. Fong, H.; Liu, W.; Wang, C.; Vaia, R. A. Polymer 2002, 43, 775.
18. Qi, Z. H.; Yu, H.; Chen, Y. M.; Zhu, M. F. Mater Lett 2009, 63, 415.
19. Miyake, A. J Polym Sci 1960, 44, 223.
20. Shenoy, S. L.; Bates, W. D.; Frisch, H. L.; Wnek, G. E. Polymer 2005, 46, 3372.
21. Gupta, P.; Elkins, C.; Long, T. E.; Wilkes, G. L. Polymer 2005, 46, 4799.
22. Mckee, M. G.; Wilkes, G. L.; Colby, R. H.; Long, T. E. Macromolecules 2004, 37, 1760.
23. Demir, M. M.; Yilgor, I.; Yilgor, E.; Erman, B. Polymer 2002, 43, 3303.
24. Lee, K. H.; Kim, H. Y.; La, Y. M.; Lee, D. R.; Sung, N. H. J Polym Sci Part B: Polym Phys 2002, 40, 2259.
25. Liu, H. Q.; Hsieh, Y. L. J Polym Sci Part B: Polym Phys 2002, 40, 2119.
26. Reneker, D. H.; Yarin, A. L. Polymer 2008, 49, 2387.